

# Chapter-4

## Antenna Arrays

*Antenna arrays* are groups of similar antennas arranged in various configurations (straight lines, circles, triangles, and so on) with proper amplitude and phase relations to give certain desired radiation characteristics. Frequently, the radiation characteristics of importance are the direction and beamwidth of the main beam, sidelobe levels, and/or directivity. In this section we examine the basic theories and characteristics of linear antenna arrays (radiating elements arranged along a straight line). The electromagnetic field of an array is the vector superposition of the fields produced by the individual antenna elements. We first consider the simplest case of two-element arrays, and then consider the basic properties of uniform linear arrays made up of many identical elements.

### 1. Two-Element Array

The simplest array, is one consisting of two identical radiating elements (antennas) spaced a distance apart. This is illustrated in Fig.9. For simplicity, let us assume that the far-zone electric field of the individual antennas be in the  $\theta$ -direction and that the antennas are lined along the x-axis. The antennas are excited with a current of the same magnitude, but the phase in antenna-1 leads that in antenna-0 by an angle  $\xi$ . We have

$$E_0 = E_m F(\theta, \phi) \frac{e^{-j\beta R_0}}{R_0}, \quad \dots (77)$$

$$E_1 = E_m F(\theta, \phi) \frac{e^{j\xi} e^{-j\beta R_1}}{R_1}, \quad \dots (78)$$

where  $F(\theta, \phi)$  is the pattern function of the individual antennas, and  $E_m$  is an amplitude function. The electric field of the two-element array is the sum of  $E_0$  and  $E_1$ . Hence,

$$E = E_0 + E_1 = E_m F(\theta, \phi) \left[ \frac{e^{-j\beta R_0}}{R_0} + \frac{e^{j\xi} e^{-j\beta R_1}}{R_1} \right]. \quad \dots (79)$$

In the far zone,  $R_0 \gg d/2$ , and the factor  $1/R_1$  in the magnitude may be replaced approximately by  $1/R_0$ . However, a small difference between  $R_0$  and  $R_1$  in the exponents may lead to a significant phase difference, and a better approximation must be used. Because the lines joining the field point  $P$  and the two antennas are nearly parallel, we may write

$$R_1 \cong R_0 - d \sin \theta \cos \phi. \quad \dots (80)$$

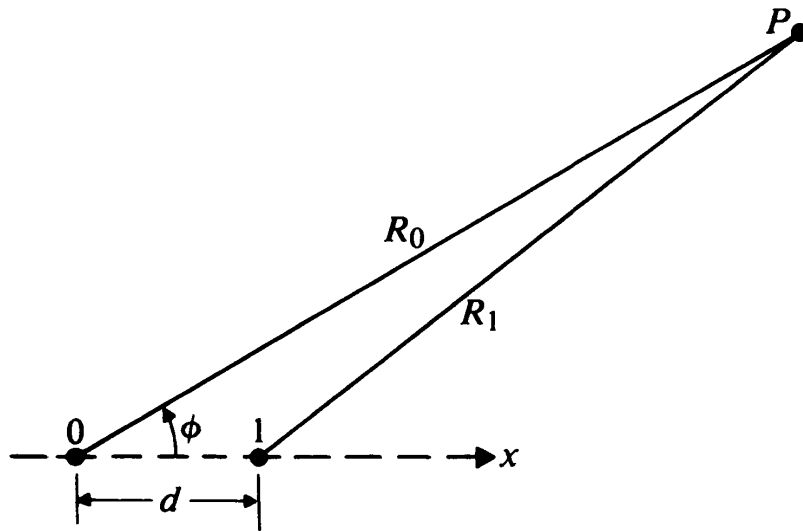


Fig.9: A two-element array

Substitution of Eq. (80) in Eq. (79) yields

$$\begin{aligned} E &= E_m \frac{F(\theta, \phi)}{R_0} e^{-j\beta R_0} [1 + e^{j\beta d \sin \theta \cos \phi} e^{j\xi}] \\ &= E_m \frac{F(\theta, \phi)}{R_0} e^{-j\beta R_0} e^{j\psi/2} \left( 2 \cos \frac{\psi}{2} \right), \end{aligned} \quad \dots (81)$$

where

$$\psi = \beta d \sin \theta \cos \phi + \xi. \quad \dots (82)$$

The magnitude of the electric field of the array is

$$|E| = \frac{2E_m}{R_0} |F(\theta, \phi)| \left| \cos \frac{\psi}{2} \right|, \quad \dots (83)$$

where  $|F(\theta, \phi)|$  may be called the *element factor*, and  $|\cos(\psi/2)|$  the normalized *array factor*. The element factor is the magnitude of the pattern function of the individual radiating elements, and the array factor depends on array geometry as well as on the relative amplitudes and phases of the excitations in the elements. (In this particular case the excitation amplitudes are equal.) The array factor is that of an array of *isotropic* elements, the directional property of the elements having been accounted for by the element factor. From Eq. (83) we may conclude that *the pattern function of an array of identical elements is described by the product of the element factor and the array factor*. This property is called the *principle of pattern multiplication*.

For an array of two parallel z-directed half-wave dipoles the magnitude of the total electric field is, from Eqs. (57) and (83),

$$|E| = \frac{2E_m}{R_0} \left| \frac{\cos [(\pi/2) \cos \theta]}{\sin \theta} \right| \left| \cos \frac{\psi}{2} \right|. \quad \dots (84)$$

Since  $\psi$  is also a function of  $\theta$ , we see that the pattern in an E-plane is not the same as that of a single dipole, except when  $\phi = \pm \pi/2$ . In the H-plane,  $\theta = \pi/2$ , and the pattern is determined entirely by the array factor  $|\cos(\psi/2)|$ .

**EXAMPLE-6:** Plot the H-plane radiation patterns of two parallel dipoles for the following two cases: (a)  $d = \lambda/2$ ,  $\xi = 0$ ; (b)  $d = \lambda/4$ ,  $\xi = -\pi/2$ .

**Solution:** Let the dipoles be z-directed and placed along the x-axis, as shown in Fig.9. In the H-plane ( $\theta = \pi/2$ ), each dipole is omnidirectional, and the normalized pattern function is equal to the normalized array factor  $|A(\phi)|$ . Thus

$$|A(\phi)| = \left| \cos \frac{\psi}{2} \right| = \left| \cos \frac{1}{2} (\beta d \cos \phi + \xi) \right|.$$

a)  $d = \lambda/2$  ( $\beta d = \pi$ ),  $\xi = 0$ :

$$|A(\phi)| = \left| \cos \left( \frac{\pi}{2} \cos \phi \right) \right|. \quad \dots (85a)$$

The pattern has its maximum at  $\phi_0 = \pm \pi/2$  —that is, in the **broadside direction**. This is a type of **broadside array**. Figure-10(a) shows this broadside pattern. Since the excitations in the two dipoles are in phase, their electric fields add in the broadside directions at  $\phi = \pm \pi/2$ . At  $\phi = 0$  and  $\pi$ , the electric fields cancel each other because the  $\lambda/2$  separation leads to a phase difference of  $180^\circ$ .

b)  $d = \lambda/4$  ( $\beta d = \pi/2$ ),  $\xi = -\pi/2$ :

$$|A(\phi)| = \left| \cos \frac{\pi}{4} (\cos \phi - 1) \right|, \quad \dots (85b)$$

which has a maximum at  $\phi_0 = 0$  and vanishes at  $\phi = \pi$ . The pattern maximum is now in a direction *along* the line of the array, and the two dipoles constitute an **endfire array**. Figure-10(b) shows this endfire pattern. In this case the phase in the right-hand dipole

lags by  $\pi/2$ , which exactly compensates for the fact that its electric field arrives in the  $\phi=0$  direction a quarter of a cycle *earlier* than the electric field of the left-hand dipole. As a consequence, the electric fields add in the  $\phi=0$  direction. In the  $\phi = \pi$  direction, the  $\pi/2$  phase lag in the right-hand dipole plus the quarter-cycle delay results in a complete cancellation of the fields.

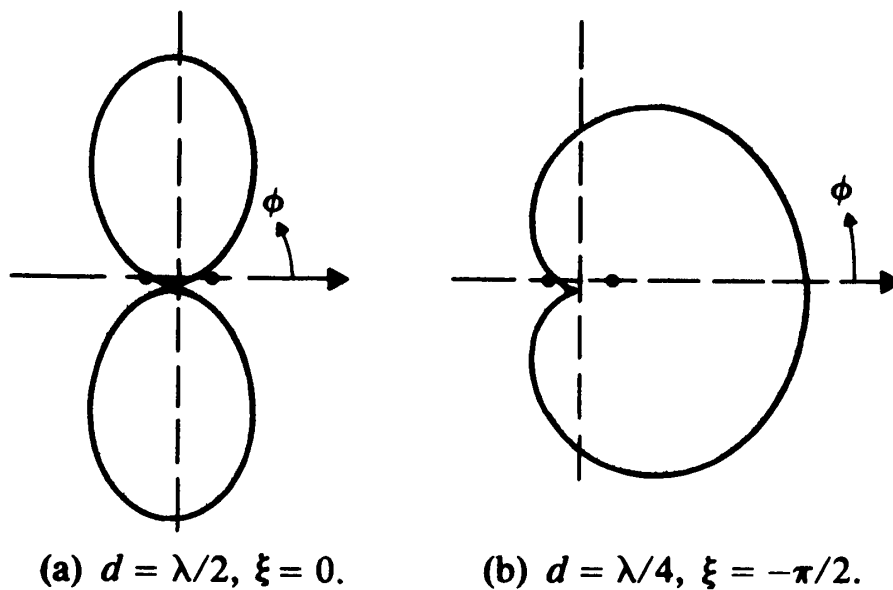


Fig.10: H-plane radiation patterns of two-element parallel dipole array.

**EXAMPLE-7:** Discuss the radiation pattern of a linear array of the three isotropic sources spaced  $\lambda/2$  apart. The excitations in the sources are in-phase and have amplitude ratios 1:2:1.

**Solution:** This three-source array is equivalent to two (two-element) arrays displaced  $\lambda/2$  from each other as depicted in Fig.11. Each (two-element) array can be considered as a radiating source with an element factor as given by Eq. (85a) and an array factor, which is also given by the same equation. By the principle of pattern multiplication we obtain:

$$|E| = \frac{4E_m}{R_0} \left| \cos \left( \frac{\pi}{2} \cos \phi \right) \right|^2. \quad \dots (86)$$

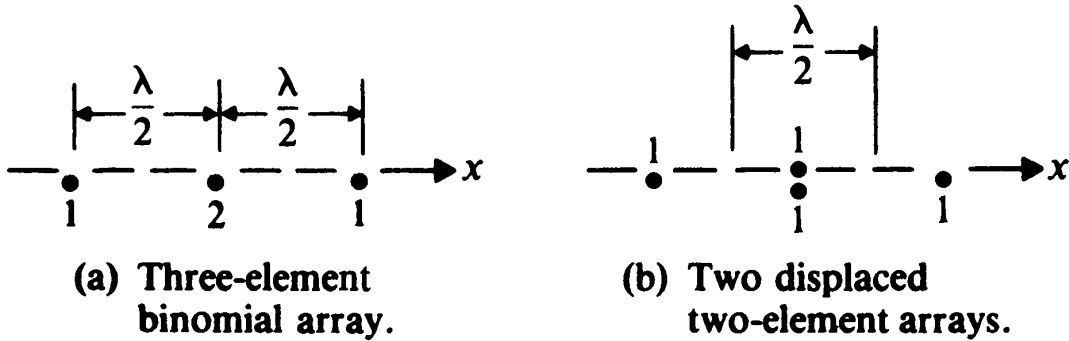


Fig.11: A three-element array and its equivalent pair of displaced two-element arrays.

The radiation pattern represented by the pattern function  $|\cos[(\pi/2) \cos\phi]|^2$  is sketched in Fig.12. Compared to the pattern of the uniform two-element array in Fig.10(a), this three-element broadside pattern is sharper (more directive). Both patterns have no sidelobes.

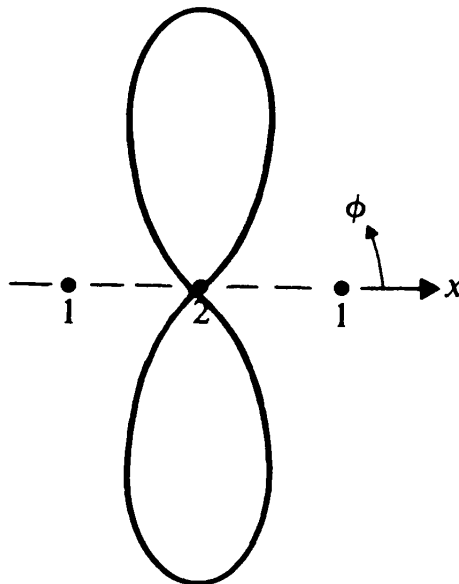


Fig.12: Radiation pattern of three-element broadside binomial array.

### ❖ Binomial Array:

The three-element broadside array is a special case of a class of *sidelobeless* arrays called *binomial arrays*. In a binomial array of  $N$  elements the excitation amplitudes vary according to the coefficients of a binomial expansion:

$$\binom{N-1}{n}, n = 0, 1, 2, \dots, N-1$$

For  $N = 3$  the relative excitation amplitudes are:

$$\binom{2}{0}=1, \quad \binom{2}{1}=2, \quad \binom{2}{2}=1 \quad \text{as in Example-7.}$$

To obtain a directive pattern without sidelobes,  $d$  in a binomial array is normally restricted to be  $\lambda/2$ . The feature of no sidelobes in the array pattern of a binomial array is accompanied by a wider beamwidth and a lower directivity compared to those of a uniform array with the same number of elements.

## 2. General Uniform Linear Arrays

We now consider an array of identical antennas equally spaced along a straight line. The antennas are fed with currents of equal magnitude and have a uniform progressive phase shift along the line. Such an array is called a *uniform linear array*. An example is shown in Fig.13, where  $N$  antenna elements are aligned along the x-axis. Since the antenna elements are identical, the array pattern function is the product of the element factor and the array factor. Our attention here will be concentrated on the manner in which the array factor depends on the parameter  $\beta d = 2\pi d/\lambda$  and the progressive phase shift  $\xi$  between neighboring elements. The normalized array factor in the xy-plane is:

$$|A(\psi)| = \frac{1}{N} |1 + e^{j\psi} + e^{j2\psi} + \dots + e^{j(N-1)\psi}|, \quad \dots (87)$$

where

$$\psi = \beta d \cos \phi + \xi. \quad \dots (88)$$

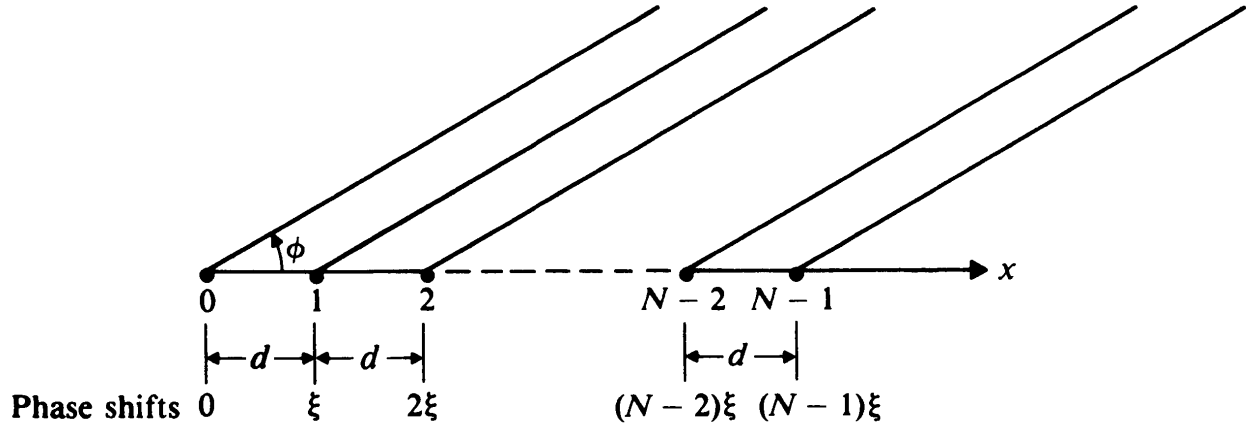


Fig.13: A general uniform array

The polynomial on the right side of Eq. (87) is a geometric progression and can be summed up in a closed form:

$$|A(\psi)| = \frac{1}{N} \left| \frac{1 - e^{jN\psi}}{1 - e^{j\psi}} \right|$$

or,

$$|A(\psi)| = \frac{1}{N} \left| \frac{\sin (N\psi/2)}{\sin (\psi/2)} \right| \quad \text{(Dimensionless).} \quad \dots (89)$$

This is the general expression of the normalized array factor for a uniform linear array. Figure-14 is a sketch of the normalized array factor for a five-element array. The actual radiation pattern as a function of  $\phi$  depends on the values of  $\beta d$  and  $\xi$ . As  $\phi$  varies from 0 to  $2\pi$ , the value of  $\psi$  changes from  $(\beta d + \xi)$  to  $(-\beta d + \xi)$ , covering a range of  $2\beta d$  or  $4\pi d/\lambda$ . This defines the visible range of the radiation pattern.

We may derive several significant properties from  $|A(\psi)|$  as given in Eq. (89).

1. **Main-beam direction:** The maximum value occurs when  $\psi=0$  or when

$$\beta d \cos \phi_0 + \xi = 0,$$

which leads to

$$\cos \phi_0 = -\frac{\xi}{\beta d}. \quad \dots (90)$$

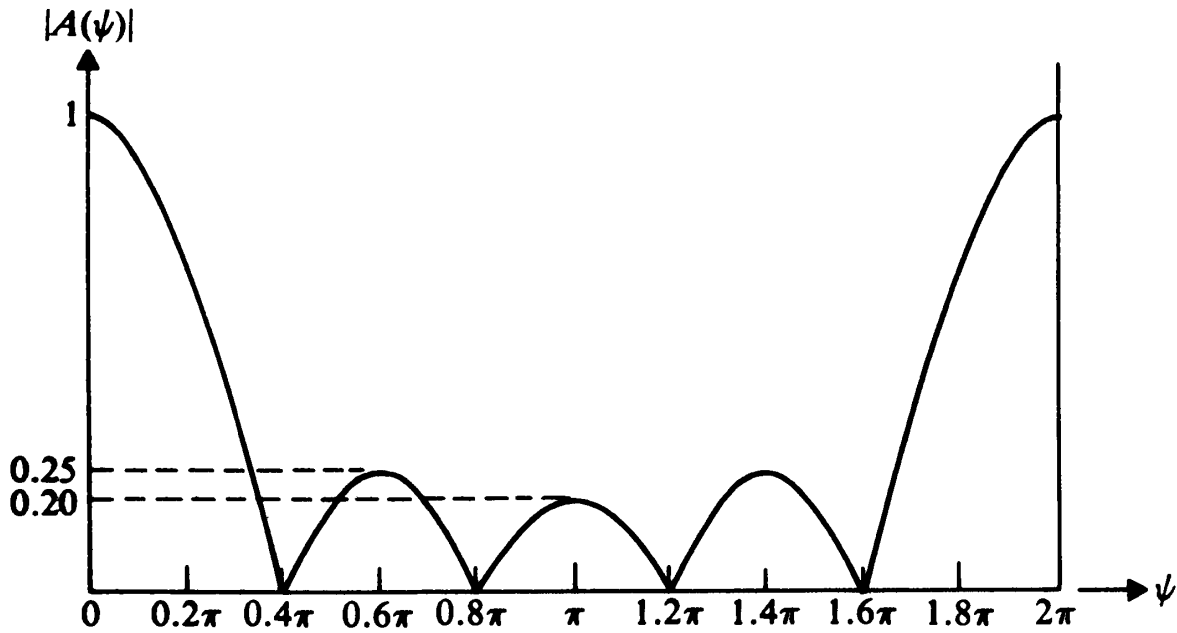


Fig.14: Normalized array factor of a five-element uniform linear array

Two special cases are of particular importance.

a) **Broadside array:** For a broadside array, maximum radiation occurs at a direction perpendicular to the line of the array—that is, at  $\phi_0 = \pm \pi/2$ . This requires  $\xi = 0$ , which means that all the elements in a linear broadside array should be excited in phase, as was the case in Example-6(a).

b) **Endfire array:** For an endfire array, maximum radiation occurs at  $\phi_0 = 0$ . Equation (90) gives:

$$\xi = -\beta d \cos \phi_0 = -\beta d.$$

We note that this condition is satisfied by the two-element array in Example-6(b).

**2. Null locations:** The array pattern has nulls when  $|A(\phi)| = 0$  or when

$$\frac{N\psi}{2} = \pm k\pi, \quad k = 1, 2, 3, \dots \quad \dots (91)$$

It is obvious that the corresponding null locations in  $\phi$  are different for broadside and endfire arrays because of the different values of  $\xi$  implicit in  $\psi$ .

**3. Beam Width of main beam:** The angular width of the main beam between the first nulls can be determined approximately for large  $N$ . Let  $\psi_{01}$  denote the values of  $\psi$  at the first nulls:

$$\frac{N\psi_{01}}{2} = \pm \pi \quad \text{or} \quad \psi_{01} = \pm \frac{2\pi}{N}.$$

In order to see how  $\psi_{01}$  converts to an angle between the first nulls in  $\phi$ , we need to know the direction of the main beam.

a) Broadside array: ( $\xi = 0, \phi_0 = \pi/2$ ). For a broadside array,  $\psi = \beta d \cos \phi$ . If the first null occurs at  $\phi_{01}$ , then the beamwidth of the main beam between the first nulls is  $2\Delta\phi = 2(\phi_{01} - \phi_0)$ . At  $\phi_{01}$  we have:

$$\cos \phi_{01} = \cos (\phi_0 + \Delta\phi) = \frac{\psi_{01}}{\beta d},$$

which, for  $\phi_0 = \pi/2$ , gives

$$\cos\left(\frac{\pi}{2} + \Delta\phi\right) = -\sin \Delta\phi = -\frac{2\pi}{N\beta d}$$

or

$$\Delta\phi = \sin^{-1}\left(\frac{\lambda}{Nd}\right) \cong \frac{\lambda}{Nd}. \quad \dots (92)$$

The last approximation is obtained when  $Nd \gg \lambda$ . Equation (92) leads to a useful rule of thumb that the width of the main beam (in radians) of a long uniform broadside array is approximately **twice** the reciprocal of the array length in wavelengths,

b) Endfire array: ( $\xi = -\beta d$ ,  $\phi_0 = 0$ ). For an endfire array,  $\psi = \beta d(\cos\phi - 1)$ , and

$$\cos \phi_{01} - 1 = \frac{\psi_{01}}{\beta d} = -\frac{2\pi}{N\beta d} = -\frac{\lambda}{Nd}.$$

But  $\cos\phi_{01} = \cos\Delta\phi \approx 1 - (\Delta\phi)^2/2$  for small  $\Delta\phi$ . Thus,

$$\frac{(\Delta\phi)^2}{2} \cong \frac{\lambda}{Nd}$$

or

$$\Delta\phi \cong \sqrt{\frac{2\lambda}{Nd}}. \quad \dots (93)$$

Comparing Eq. (93) with Eq. (92), we may conclude that the width of the main beam of a uniform endfire array is greater than that of a uniform broadside array of the same length (because  $Nd > \lambda/2$ ).

**4. Sidelobe locations:** Sidelobes are minor maxima that occur approximately when the numerator on the right side of Eq. (89) is a maximum—that is, when  $|\sin(N\psi/2)| = 1$  or when:

$$\frac{N\psi}{2} = \pm(2m + 1) \frac{\pi}{2}, \quad m = 1, 2, 3, \dots \quad \dots (94)$$

The first sidelobes occur when

$$\frac{N\psi}{2} = \pm \frac{3}{2} \pi, \quad (m = 1). \quad \dots (95)$$

Note that  $N\psi/2 = \pm \pi/2$  ( $m = 0$ ) does not represent locations of sidelobes because they are still within the main-lobe region.

**5. First sidelobe level:** An important characteristic of the radiation pattern of an array is the level of the first sidelobes compared to that of the main beam, since the former is usually the highest of all sidelobes. All sidelobes should be kept as low as possible in order that most of the radiated power be concentrated in the main-beam direction and not be diverted to sidelobe regions. Substituting Eq. (95) in Eq. (89), we find the amplitude of the first sidelobes to be (for large  $N$ ):

$$\frac{1}{N} \left| \frac{1}{\sin(3\pi/2N)} \right| \cong \frac{1}{N} \left| \frac{1}{3\pi/2N} \right| = \frac{2}{3\pi} = 0.212$$

In logarithmic terms the first sidelobes of a uniform linear antenna array of many elements are  $[20 \log_{10} (1/0.212)]$  or  $[13.5 \text{ (dB)}]$  down from the principal maximum. This number is almost independent of  $N$  as long as  $N$  is large.

❖ **Tapered Current Distribution:**

One way to reduce the sidelobe level in the radiation pattern of a linear array is to taper the current distribution in the array elements—that is, to make the excitation amplitudes in the elements in the center portion of an array higher than those in the end elements. This method is illustrated in the following example.

**EXAMPLE-8:** Find the array factor and plot the normalized radiation pattern of a broadside array of five isotropic elements spaced  $\lambda/2$  apart and having excitation amplitude ratios 1:2:3:2:1. Compare the first sidelobe level with that of a five-element uniform array.

**Solution:** The normalized array factor of the five-element tapered array is:

$$\begin{aligned}
 |A(\psi)| &= \frac{1}{9} |1 + 2e^{j\psi} + 3e^{j2\psi} + 2e^{j3\psi} + e^{j4\psi}| \\
 &= \frac{1}{9} |e^{j2\psi} [3 + 2(e^{j\psi} + e^{-j\psi}) + (e^{j2\psi} + e^{-j2\psi})]| \\
 &= \frac{1}{9} |3 + 4 \cos \psi + 2 \cos 2\psi|. \quad \dots (96)
 \end{aligned}$$

The graph of  $|A(\psi)|$  versus  $\psi$  is shown in Fig.15(a). Note that this figure holds for a general  $\psi = \beta d \cos \phi + \zeta$ ; the values of  $\beta d$  and  $\zeta$  have not yet been specified.

In order to plot the desired radiation pattern we use the following additional information:

$$\begin{aligned}
 \text{Broadside radiation, } \zeta = 0: \quad \psi &= \beta d \cos \phi; \\
 \text{Element spacing, } d = \frac{\lambda}{2}: \quad \psi &= \pi \cos \phi.
 \end{aligned}$$

The normalized radiation pattern can be plotted from:

$$|A(\phi)| = \frac{1}{9} |3 + 4 \cos (\pi \cos \phi) + 2 \cos (2\pi \cos \phi)|.$$

However, having calculated and plotted  $|A(\psi)|$ , we do not need to recalculate the array factor as a function of  $\phi$ . This conversion can be effected graphically as follows (see Fig.15):

1. Extend the vertical axis of the array factor graph downward, and let it intersect with a horizontal line (which represents the line for  $\phi=0$  and  $\phi=\pi$ ).The point of intersection is the point for  $\xi =0$ .

2. Locate the point  $P_o$  on the horizontal line that is  $\xi$  radians to the right or left of the point of intersection, depending on whether  $\xi$  is positive or negative. (In the present case,  $\xi = 0$  and  $P_o$  is at the point of intersection).
3. Using  $P_o$  as the center, draw a circle with  $\beta d$  as the radius.
4. For any angle  $\phi_1$ , draw the radius vector  $P_o P_1$  (The projection  $P_o P_1'$  is equal to  $\psi_1 = \beta d \cos \phi_1$ )
5. At  $\psi_1$ , measure the magnitude of  $|A(\psi_1)|$ , which is marked as  $P_2$  on the radius vector  $P_o P_1$  ( $P_2$  is a point on the normalized radiation pattern.)

Repeat this process until the entire radiation pattern is obtained.

Figure-15(b) shows the normalized radiation pattern of this five-element broadside array with tapered excitation. The first sidelobe level is found to be 0.11 or  $[20 \log_{10}(1/0.11) = 19.2 \text{ (dB)}]$  down from the main-beam radiation. This compares with 0.25 or 12 (dB) down for the five-element uniform broadside array shown in Fig.14.

In the discussion of uniform linear arrays we started out with the assumptions of equal spacing, equal excitation amplitude, and constant progressive phase shifts. The main reason for making these assumptions is mathematical simplicity in analyzing radiation characteristics. The preceding example shows that a tapered nonuniform amplitude distribution in the array elements produces the desirable result of a reduction in the sidelobe level. In a similar manner the spacings between neighboring elements may be made unequal, and the phase shifts do not have to be constant. In two-dimensional arrays the elements need not be arranged in a rectangular lattice. We have, then, many additional parameters that can be adjusted to achieve desirable results. Adjustments in these parameters, however, destroy the simplicity of the analysis. There are techniques for synthesizing an antenna array to approximate a specified radiation pattern closely. It

is not possible to examine all the various possible array designs in this chapter, but they do exist and present themselves as interesting problems.

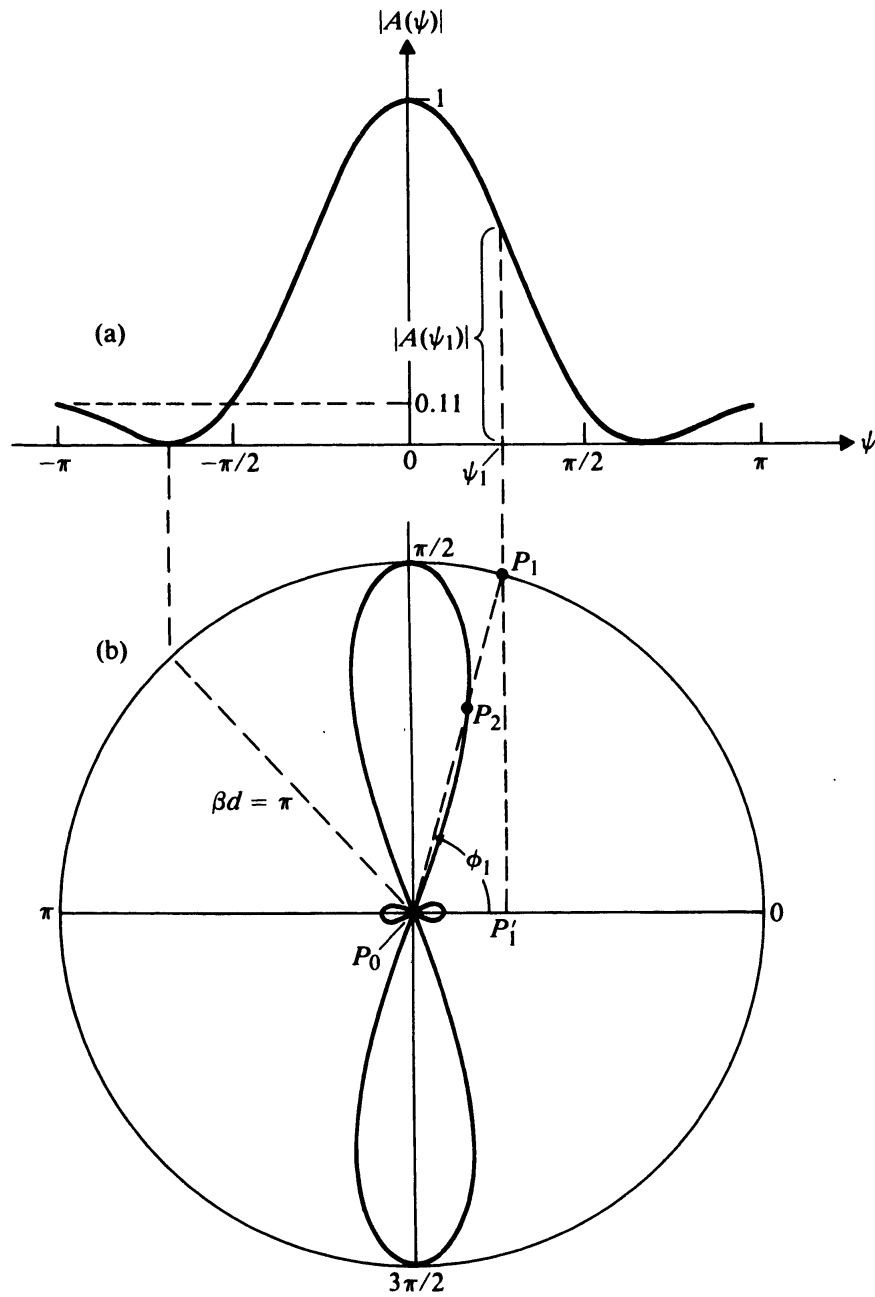


Fig.15: Graph for normalized array factor as a function of  $\psi$ , and normalized polar radiation pattern of a five-element broadside array with  $d = \lambda/2$  and tapered excitation amplitude ratios 1:2:3:2:1 (Example-8).

Our discussions on linear arrays can be extended to two-dimensional rectangular arrays. A rectangular array can be studied as an array of linear arrays, to which the principle of pattern multiplication applies. From Eq. (90) we note that the direction of the main beam of a uniform linear array can be changed by simply changing the amount of progressive phase shift  $\xi$ . In fact, the radiation pattern can be changed from broadside ( $\xi=0$ ) to endfire ( $\xi = -\beta d$ ) or to somewhere in between. We see here a possibility of *scanning* the main beam by simply varying  $\xi$ . This can be achieved in practice by using electronically controlled phase shifters. Antenna arrays equipped with phase shifters to steer the main beam electronically are called *phased arrays*. The main beam of a two-dimensional array can be made to scan in both  $\theta$  (elevation) and  $\phi$  (azimuth) directions. Scanning phased arrays are of great practical importance in radar and radioastronomy work, in which the antenna system may be arrays of many thousands of elements that are not amenable to rapid mechanical motion for beam steering. Time-delay circuits may also be used to furnish the required phase shifts to the various array elements. By changing the frequency the time-delays are translated into varying phase shifts. This scheme is called *frequency scanning*.